Journal of Constructional Steel Research 210 (2023) 108069

Contents lists available at ScienceDirect

Journal of Constructional Steel Research

journal homepage: www.elsevier.com/locate/jcsr

Experiments and proposed model for residual stresses in hot-rolled wide flange shapes

Andronikos Skiadopoulos, Albano de Castro e Sousa, Dimitrios G. Lignos *

School of Architecture, Civil and Environmental Engineering, École Polytechnique Fédérale de Lausanne (EPFL), Station 18, Lausanne 1015, Switzerland

ARTICLE INFO

Keywords:
Residual stresses
Hot-rolled steel profiles
Statistical analyses
Dataset
Residual stress measurements
Wide flange shapes

ABSTRACT

This paper proposes a new residual stress model for hot-rolled wide flange steel cross sections. For this purpose, a dataset of 85 residual stress measurements is first assembled. The dataset is comprised of prior measurements available in the literature that are complemented by additional ones as part of the present study. A constrained optimization problem is then formulated by assuming parabolic residual stress distributions for both the flanges and the web of hot-rolled wide flange cross sections. The parameters of the developed residual stress model are inferred from the results of the optimization method and from rigorous statistical analyses. The results demonstrate that the cross-sectional area and the depth-to-width ratio strongly influence the residual stress distributions in the flanges and the web of a hot-rolled wide flange profile. The results suggest that there is no evidence that the yield strength of the material influences the developed residual stresses within a cross section. Contrary to available residual stress models in the literature that may be applicable for a limited range of cross-sectional geometries, the proposed model reduces the mean error between all available measurements and predictions by 60%–70%. The variance of the error is also reduced by a factor of two to four across all known cross-sectional properties.

1. Introduction

Residual stresses form during the manufacturing process of structural steel members. They are attributed to uneven cooling, welding, and/or cold forming [1]. In the former two cases, residual stresses are formed as a result of differential cooling rates. In the case of cold forming, residual stresses are attributed to uneven spatial inelastic strain distributions [2].

In the casting process of wide flange cross sections, the flange plate edges and the web center tend to cool down earlier than the web-to-flange joint. These early cooling regions increase their Young's modulus faster than their neighboring areas which, in effect, restrain the shrinking of the warmer parts of the cross section. As such, in built-up or hot-rolled cross sections the late cooling web-to-flange joint is subjected to tensile stresses and the flange tip and the web center that cool earlier are subjected to compressive stresses to satisfy the equilibrium within the cross section (see Fig. 1). If, however, web cooling is delayed, the web can be subjected to pure tension [1]. The effect of cooling rate on residual stresses was also stressed by Mas [3], where slow cooling rates were related with decreased residual stresses within the cross section. In built-up cross sections, residual stresses are typically higher compared to those in hot-rolled sections due to the high temperature gradient spatial distributions during plate welding that accelerates plate cooling [4].

Residual stresses depend mainly on the geometry of hot-rolled wide flange cross sections, the rolling temperature, the cooling process and the cold straightening [1,5–10]. They are typically assumed to follow a parabolic distribution [11,12], as schematically depicted in Fig. 1b. Hereinafter, tensile stresses are denoted with a plus sign and compressive ones with a minus sign. The material yield strength was not found to affect the overall pattern and magnitude of the residual stresses [1,5–11,13]. As such, for a given cross-sectional geometry, members made of mild structural steel are expected to yield earlier than those made of high strength steel, i.e., the effect of residual stresses on mild steel is more significant compared to high strength steel.

The presence of residual stresses in hot-rolled structural steel members could lead to premature yielding and/or may accelerate the onset of geometric instabilities [14]. Moreover, it may accelerate corrosion, brittle fracture and fatigue [14]. The influence of residual stresses on reducing the lateral load capacity of hot-rolled steel members was identified in the early 1950s from experimental research on columns [7,15]. This was confirmed by subsequent studies on structural steel members [4,10,16–18]. The presence of residual stresses influences the resistance of a structural steel member against lateral–torsional and

* Corresponding author.
E-mail addresses: andronikos.skiadopoulos@epfl.ch (A. Skiadopoulos), albano.sousa@epfl.ch (A. de Castro e Sousa), dimitrios.lignos@epfl.ch (D.G. Lignos).

https://doi.org/10.1016/j.jcsr.2023.108069
Received 27 February 2023; Received in revised form 9 June 2023; Accepted 12 June 2023
Available online 27 June 2023

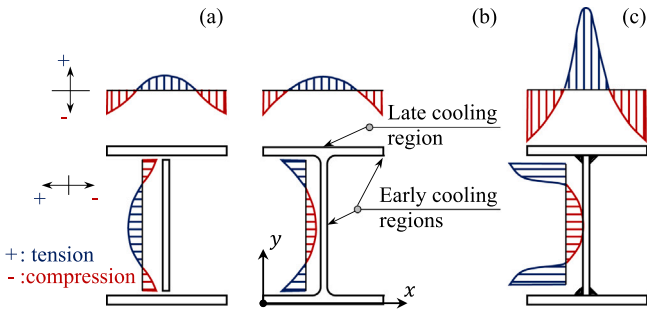

Fig. 1. Formation of residual stresses in: (a) steel plates; (b) hot-rolled steel cross sections; and (c) built-up steel cross sections.

flexural buckling [19–21]. This is attributed to the premature yielding as well as the increase of the Wagner coefficient [7,22] in the presence of residual stresses. Residual stresses strongly influence the buckling resistance of members under high compressive axial loads [23,24] and intermediate normalized member slenderness, ranging from 0.5 to 1.2 [25].

When hot-rolled or built-up sections do not meet the initial geometric imperfection requirements [26–28], cold straightening is employed. This process entails further redistribution of residual stresses within a structural member [29–31] that alters those formed after welding and/or hot-rolling. As a result, residual stresses may vary within a structural member and may even be asymmetrical in case of cold straightening along the weak axis of the cross section [32,33].

All-in-all, the magnitude and shape of residual stresses depend on many parameters and estimating them precisely *a priori* may be challenging [18,34,35]. Regardless of the existing variability in the way residual stresses develop, prior work focused on the development of simplified residual stress models for non-straightened hot-rolled wide flange cross sections [4,7,11,12,36,37]. Since the buckling resistance of wide flange members is mainly provided by the flanges, emphasis was put in the flange residual stresses [38].

Bradford and Trahair [36] assumed parabolic residual stress distributions in the flanges, with fixed values at the mid-flange and flange tip locations of $0.5f_y$ and $-0.35f_y$ (where f_y is the material yield strength), respectively, regardless of the section geometry. With regards to the residual stresses in the web, a quartic distribution was assumed, with peak values relying on A_f, A_w, h, t_f, and b_f (where A_f and A_w are the areas of the flanges and the web, respectively, and h, t_f and b_f are the height, the flange thickness and flange width of the cross section, respectively). The model proposed by Szalai and Papp [12] is similar in nature with that of Bradford and Trahair [36] except from the fact that the residual stresses in the web are assumed to follow a parabolic distribution. Both models suggested that residual stresses are proportional to f_y and constrained the Wagner coefficient to zero. This implies that there is no torque due to residual stresses after a member is loaded, thereby suggesting no reduction in the torsional stiffness of the steel member.

Galambos and Ketter [7] suggested that the web is under pure tension for compact cross sections featuring $h/b_f < 1.5$. They proposed a fixed residual stress distribution for the flanges that relies on f_y. Young [11] proposed parabolic residual stress distributions for the flanges and the web of primarily light-to-medium weight wide flange cross sections (i.e., $19 \leq W \leq 280$ kg/m, where W is the cross-sectional weight per meter). Interestingly, the proposed distributions do not depend on f_y in this case.

Although a single geometric parameter cannot depict the residual stress distributions in the flanges and the web of a cross section, numerous models still rely on this assumption. For instance, Young [11] selected the A_w/A_f ratio for their one-parameter model. Other studies [8,10,13,38,39] lean on a trend of the peak web and flange residual stresses with respect to $(b_f/t_f)/(d_w/t_w)$ (where d_w is the depth of straight portion of the web and t_w is the web thickness of the cross section). The role of the h/b_f parameter was also stressed by the European Convention for Constructional Steelwork (ECCS) [4]. In stocky cross sections with $h/b_f < 1.2$, higher residual stresses are expected because the flange and the web plates are subjected to an increased confinement. More recently, Spoorenberg [30] showed qualitatively that cross sections with smaller area develop considerably lower residual stresses compared to sections with a larger area.

Comparisons of experimental data with finite element models that disregard residual stresses show that the flexural resistance of steel members that are prone to lateral–torsional buckling may be underestimated by about 30% [40]. Moreover, the difference in predicting the lateral–torsional buckling resistance by considering different available residual stress models may exceed 20% [40]. As per Eurocode 3 [28], the flexural and lateral–torsional buckling equations are based on finite element simulations that utilized the ECCS residual stress model [4], which is found to underestimate the member buckling resistance [41]. Contrary to this conservative approach, the lateral–torsional buckling resistance of steel members according to the US specifications is based on experimental data [42].

The development of available residual stress models to date was mostly based on calibrations to limited experimental data that date back to 1950s–1970s. The validity of these models in estimating residual stress profiles in wide flange steel cross sections that are produced with current fabrication techniques and quality control has not been assessed to date. An improved residual stress model for hot-rolled wide flange cross sections is timely, similarly to recent developments on built-up cross sections [43].

To address the existing knowledge gap, this paper proposes a new residual stress model for hot-rolled wide flange cross sections as part of non-straightened steel members. First, available residual stress models in literature are evaluated based on data from 85 residual stress measurements that are collected in a consistent format. Out of these data, 21 correspond to steel members manufactured after 2010, while the remaining ones were manufactured before 1992. The assembled residual stress dataset is supplemented by measurements conducted by the authors to acquire information on cross-sectional geometries for which measurements are lacking. A constrained least square problem is then formulated based on parabolic distributions for the flanges and the web and applied to the assembled dataset. A new residual stress model is then developed based on rigorous statistical analyses.

2. Available residual stress data for hot-rolled cross sections

Table 1 summarizes the available data from residual stress measurements. The dataset comprises measurements of various steel grades from US, British, Canadian, European and Italian manufacturers that date from 1958 to 2021. The nominal yield strength, $f_{y,n}$, ranges from 235 MPa to 460 MPa. With regards to the geometric properties, the dataset consists of cross sections with height to width ratio, h/b_f, that ranges from 1.0 to 3.0, and flange thickness, t_f, from 5.7 mm to 130 mm. The dataset is made publicly available at [44]. Residual stress measurements were mostly conducted between 1950s and 1970s [6,10,11,13,22,32,38,45,46]. Regarding the residual stress measurements of the assembled dataset, flange and web centerline measurements are reported. When residual stresses are reported through the thickness of the flange or the web plate, the average residual stresses thought the plate thickness are extracted (e.g., [37]).

Fig. 2 shows the available European profiles and the collected data with respect to the geometric properties that affect the residual stresses within a hot-rolled wide flange cross section [4,11]. From this figure, the collected data cover a broad range of the European profiles. Referring to the web local slenderness ratio, d_w/t_w, available residual stress data range from 3.0 to 54.0, while the flange local slenderness ratio, $b_f/2t_f$, ranges from 1.3 to 9.4. However, there is still need for

Table 1
Summary of collected residual stress experimental data on hot-rolled cross sections (in alphabetical order).

Reference	Year	Nr. tests	Steel grade	$f_{y,n}$ [MPa]	h/b_f	t_f [mm]
Adams et al. [45]	1964	2	ASTM A441	345	1.0–1.2	11.0-18.0
Albert et al. [47]	1992	2	300 W	300	1.9–2.8	9.7-10.7
Alpsten [13]	1968	3	ASTM A7	250	1.9–2.7	11.2-21.1
Auger [48]	2017	1	ASTM A992 Gr50	345	1.0	19.6
Brozzetti et al. [46]	1970	1	ASTM A36	250	1.3	124.7
Daddi and Mazzolani [32]	1971	23	Fe 42C	235	1.0–2.0	8.0-39.0
de Castro e Sousa and Lignos [49]	2017	3	S355-J2	355	1.1–2.2	13.5-39.0
Dibley [22]	1969	4	DL30	380	1.0–3.0	8.4-20.6
Dux and Kitipornchai [50]	1983	1	Not Reported	250	1.8	10.9
Feder and Lee [6]	1959	3	ASTM A242	345	1.0–1.5	11-16.3
Jez-Gala [38]	1962	4	Not Reported	250	1.0	9.3-21.7
Ketter [10]	1958	11	ASTM A7	250	1.0–3.0	5.7-77.2
Lamarche and Tremblay [19]	2011	1	ASTM A992 Gr50	345	1.0	20.6
Spoorenberg et al. [30]	2010	7	S235/S355	235/355	1.0–2.1	8.0-22.5
Spoorenberg et al. [37]	2013	6	HISTAR 460	460	1.2–2.3	115.0-130.0
Sonck et al. [51]	2013	1	S275	275	2.0	7.4
Tankova et al. [52]	2021	2	S460	460	1.0–2.5	15.5-16.0
Young [11]	1975	5	BS-4360 Gr43A	250	1.0–2.3	6.6-11.2
Present study	2021	5	S355-J2	355	1.0–2.1	6.3-40.0
Total	–	85	–	235–460	1.0–3.0	5.7-130.0

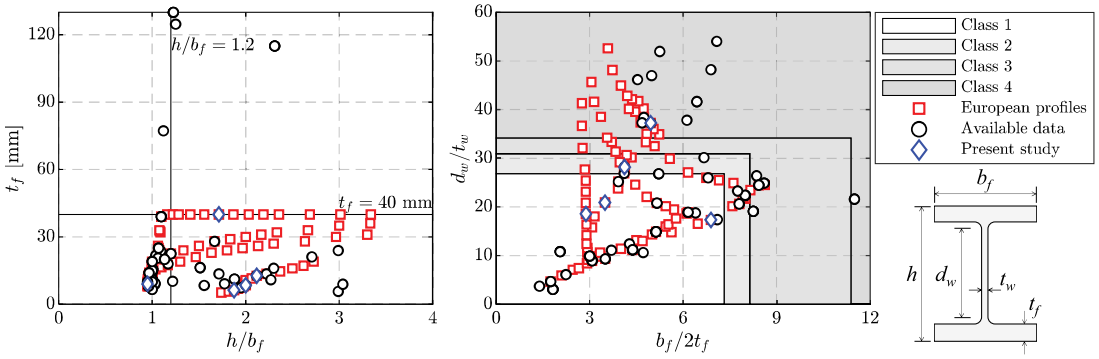

Fig. 2. Available residual stress experimental data with respect to cross-sectional geometric properties.

supplementary residual stress data to better describe the $b_f/2t_f - d_w/t_w$ space, especially for cross sections with $b_f/2t_f \sim 3.0-4.0$ and $d_w/t_w \sim 10.0-30.0$. The cross-sectional classification for pure axial compression and $f_{y,n} = 355$ MPa is superimposed in the same figure. Most cross sections (i.e., nearly 70 out of the 85) are Class 1 and 2 according to [28]. For the remaining cross sections, plastic analysis would only be permissible under combined compression and bending [28].

3. Assessment of residual stress models for hot-rolled cross sections

Fig. 3 shows comparisons of available residual stress measurements with the corresponding residual stress model predictions. Particularly, predictions are based on the models by Bradford and Trahair [36], ECCS [4], Galambos and Ketter [7], Szalai and Papp [12] and Young [11]. Fig. 3a features an IPE 400 European cross section made of S355-J2 mild steel (i.e., $f_{y,n} = 355$ MPa), while Fig. 3b features a W14 × 808 US cross section made of HISTAR 460 high strength steel (i.e., $f_{y,n} = 460$ MPa). The former section is a relatively deep one, with $(b_f t_w)/(d_w t_f) = 0.3$, while the latter section is a stocky one, with $(b_f t_w)/(d_w t_f) = 0.6$.

Referring to the Galambos and Ketter model [7], it was based on light-weight sections, where residual stresses in the web can be primarily in tension [13,29]. For heavier sections, as those in Fig. 3, this assumption may not hold true [13,29], because the web is primarily in compression and residual stresses seem to follow a parabolic distribution. The residual stress model by Young [11] was developed based on light-to-medium weight cross sections. This model provides reasonable predictions for cross sections with $(b_f t_w)/(d_w t_f) < 0.5$ that are common for steel beams in buildings. With regards to Bradford and Trahair [36], it overestimates the mid-flange residual stresses for the high-strength steel cross section of Fig. 3b. Similarly to [4,7,12], this model relies on f_y, by assuming constant mid-flange tensile residual stresses equal to $0.5f_y$, regardless of the cross-sectional geometry. Moreover, the quartic residual stress distribution in the web is not justifiable.

The Szalai and Papp model [12] assumes the Wagner coefficient to be equal to zero and leads to erroneous residual stress distributions in the web, especially for stocky sections, whose torsional stiffness is appreciable [49]. There is no scientific justification for setting the Wagner coefficient equal to zero [40]. Finally, the ECCS model [4] is not generally applicable, because it relies on f_y and is independent to the cross-sectional geometry. Moreover, the assumed linear distribution does not accurately describe the residual stress evolution within the flange and web plates.

To assess the predictive capability of available residual stress models, the L1-norm (namely Manhattan norm) is calculated for the difference between available model predictions (i.e., [4,7,11,12,36]) and residual stress measurements. The L1-norm is calculated for both the flanges and the web, as per Eqs. (1a) and (1b), accordingly:

$$\|(x^f_{model} - x^f_{real})\| = \sum_{0}^{b_f} |(x^f_{i,model} - x^f_{i,real})| \tag{1a}$$

$$\|(y^w_{model} - y^w_{real})\| = \sum_{t_f}^{h-t_f} |(y^w_{i,model} - y^w_{i,real})|, \tag{1b}$$

where $x^f_{i,real}$ and $y^w_{i,real}$ are the measured residual stresses in the flange and the web, accordingly, at a location i of the flange and the web

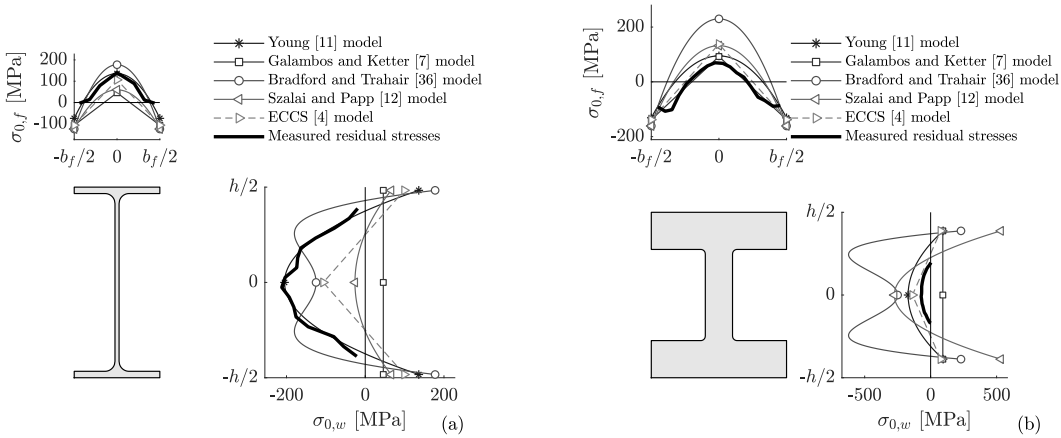

Fig. 3. Comparisons of representative residual stress measurements with available residual stress models: (a) IPE 400, [49]; and (b) W14 × 808, [37].

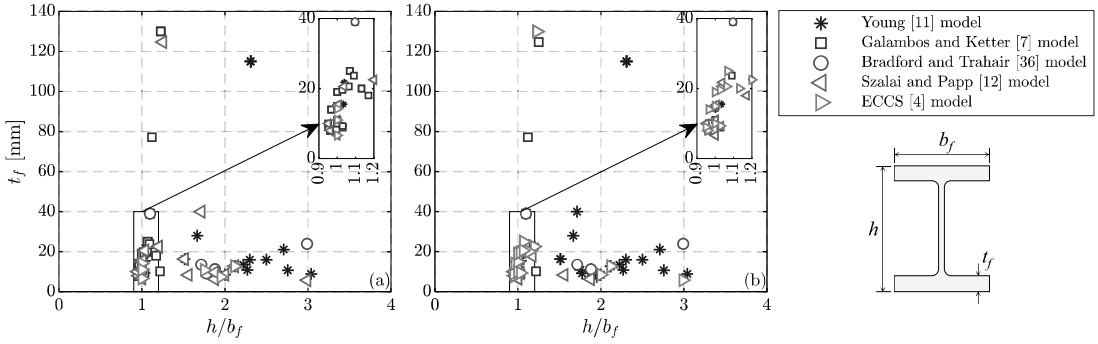

Fig. 4. Minimum L1-norm residual stress model predictions for available experimental data with respect to t_f and h/b_f: (a) flange; and (b) web.

plates, whereas $x^f_{i,model}$ and $y^w_{i,model}$ are the corresponding residual stress predictions based on available residual stress models.

Fig. 4 shows the best performing model at each of the data points. Specifically, Fig. 4 depicts the residual stress models with the minimum L1-norm for all available residual stress data with respect to t_f and h/b_f, which are the main geometric variables of the ECCS [4] model. For relatively slender cross sections with $h/b_f > 1.5$, the Young model [11] describes best the residual stresses for both the flange and the web of a hot-rolled wide flange cross section. This agrees with past studies [49]. For stocky cross sections with $h/b_f \leq 1.5$, it is inconclusive which model provides the least error for the flanges and the web.

4. Experimental program

4.1. Profile selection

To further extend the collected dataset, five additional residual stress measurements on hot-rolled wide flange cross sections are conducted, according to the sectioning method [53,54]. The steel members are made of S355-J2 mild steel with $f_{y,n} = 355$ MPa. The selected cross sections are summarized in Table 2 and are depicted in Fig. 5 prior and after section slicing.

A first objective of the experimental program is to measure residual stresses on Class 1 sections with $b_f/2t_f \sim 3.0 - 4.0$ and $d_w/t_w \sim 10.0 - 30.0$. For this purpose, an IPE 120 (i.e., $b_f/2t_f = 3.5$ and $d_w/t_w = 20.9$) and an HEM 500 (i.e., $b_f/2t_f = 2.88$ and $d_w/t_w = 18.6$) profiles were selected. A second objective is to investigate the influence of the steel grade on residual stresses. To achieve this, measurements on an IPE 200 and an IPE 360 were conducted for the steel material with $f_{y,n} = 355$ MPa to compare these with available measurements on the same profiles for steel materials with $f_{y,n} = 235$ MPa [30,32]. Finally, to investigate how regional aspects with different manufacturing techniques affect the residual stresses, measurements were conducted for an HEA 160 European profile. These measurements were compared with those of an equivalent W6 × 20 US profile [22].

4.2. Available residual stress measurement methods

Residual stresses are experimentally measured either by destructive or non-destructive methods [55,56]. The former mechanical stress-relaxing category comprises mainly the hole-drilling technique, the deep hole method, the slicing technique and the sectioning method among others. The latter relies mostly on diffraction techniques. Although the above methods provide fairly accurate results, they necessitate specialized equipment and they are generally applicable for small scale specimens. Contrary to that, the destructive methods, do not require specialized equipment and they do not compromise the accuracy of measurements.

Among the methods described herein, some measure residual stresses locally (e.g., diffraction methods and the hole-drilling technique) and some utilize extensiometers over a gage length of 100–250 mm (i.e., the slicing technique and the sectioning method). In the latter case, averaging of the residual stresses over the gage length is required. Such methods have been found to provide satisfactory results for structural steel cross sections [11,38].

In the present study, the sectioning method is selected instead of the slicing one, since the variation of residual stresses through the thickness direction of hot-rolled wide flange steel sections is insignificant [37]. Besides, most of the available residual stress measurements on hot-rolled wide flange cross sections employed sectioning.

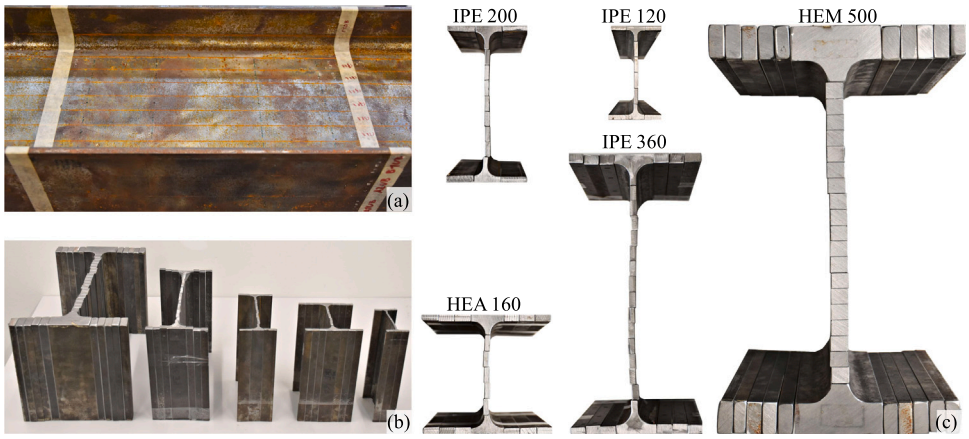

Fig. 5. (a) Markings prior to slicing (IPE 200); (b) side view of sliced cross sections; and (c) plan view of sliced cross sections (in scale).

Table 2
Summary of experimental residual stress measurements.

Profile	Steel grade	$f_{y,n}$ [MPa]	A [mm^2]	h/b_f	t_f [mm]	$b_f/2t_f$	d_w/t_w
IPE 120	S355-J2	355	1320	1.88	6.3	3.49	20.9
HEA 160	S355-J2	355	3880	0.95	9.0	6.89	17.3
IPE 200	S355-J2	355	2850	2.00	8.5	4.12	28.2
IPE 360	S355-J2	355	7270	2.12	12.7	4.96	37.3
HEM 500	S355-J2	355	34400	1.71	40.0	2.88	18.6

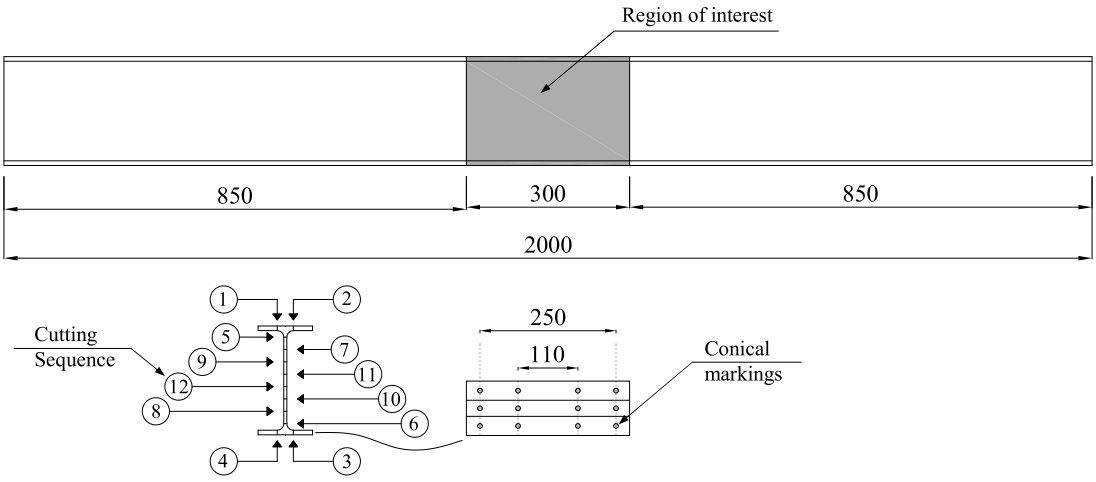

Fig. 6. Schematic of the region of interest, slice cutting sequence and reference length conical marking locations for the IPE 200 cross section (unit: millimeters).

4.3. Methodology for residual stress measurements

The sectioning method relies on the release of the residual stresses in the longitudinal-direction slices that the section is divided into, as illustrated in Fig. 6. The transverse stresses are assumed to be negligible in this case [53]. The longitudinal residual stresses are deduced by applying the Hooke's law in the slices. To achieve this, the change in the length of the slices is measured before and after slicing. The number of the selected slices in the cross section depends on the residual stress gradient. However, given that the cold sawing process of slicing usually removes 2–3 mm of material, a minimum slice width of 20 mm is necessary.

The measurements were extracted over the cross section region of interest (see Fig. 6). This region was defined by the largest gage measurement length of the slices plus 50 mm [57] and was carefully protected throughout the slicing and measurement process by applying a protective compound. Since the present study investigates residual stresses due to hot-rolling, cold-straightening was not applied in the steel member. The specimens were cut 850 mm away from the region of interest at both ends (see Fig. 6). This length respects the minimum length of $1.5b_f$ proposed by Ziemian [57] to avoid heat-induced modification of the residual stresses due to the cold-sawing process of cutting the specimen in the region of interest. The adopted cutting sequence of the slices for a characteristic cross section is illustrated in Fig. 6. However, the sequence of slicing is not expected to influence the residual stress measurements, as long as the self-equilibriate section state does not lead to slice yielding [53].

Gage lengths of 110 mm and 250 mm were utilized for redundancy in the measurements. The measured slice length was determined by the average of six measurements (i.e., three measurements per slice surface) per gage length. A 250 mm measuring base extensiometer was utilized for the measurements, with a 0.005 mm system accuracy. Since the utilized extensiometer featured a ball tip, the specimen markings that define the gage length were conducted with the aid of a conical head, so as the extensiometer rests precisely in the indentations. Even though both gage length measurements showed a good agreement, the measurements extracted from the 250 mm one were deemed more

accurate. Therefore, the residual stress results reported in the present study represent the 250 mm gage length measurements.

The longitudinal residual stresses were obtained according to Eq. (2). The minus sign in Eq. (2) indicates that in case of slice expansion, the residual stresses are compressive. Corrections were applied for curvature and temperature differences in measurements before and after slicing. As for the former correction, this was applied to correct the cord length measurements of the curved slices to arc gage lengths, according to Eq. (3). The slices remained fairly flat after slicing, except from those extracted near the k-area of the cross section. Nearby this region, the stresses differed substantially in the two slice surfaces. Therefore, except from a few cases, the curvature correction factor did not lead to appreciable modifications in the residual stresses computed directly from the Hooke's law. This suggests that the through-thickness residual stresses were insignificant [57], as the sectioning method assumes. As for the temperature difference correction, the temperature was measured at each gage length measurement instance, before (noted as T_0) and after (noted as T) slicing. In case of positive temperature difference, $T-T_0 > 0$, expansion of the gage length by ΔL is predicted according to Eq. (4). The maximum temperature difference in the testing program of the present study was +3°C, which corresponds to an overestimation of the residual stresses by up to +7 MPa in case the temperature correction is neglected.

$$\sigma_r = -E\epsilon, \text{ where } \epsilon = \frac{L_f - L_0}{L_0} \tag{2}$$

$$L_f = \theta R, \text{ where: } \theta = 2arcsin(\frac{\bar{L}_f}{2R}) \text{ and } R = \frac{4f^2+\bar{L}_{dev}}{8f} \tag{3}$$

$$\Delta L = \alpha L_0 (T - T_0) \tag{4}$$

Where σ_r is the measured residual stress in the slice, E is the Young's modulus, which is assumed to be 210 GPa, ϵ is the uniaxial strain in the slice, which is measured within the gage length, L_0 is the gage length prior to slicing, L_f is the arc gage length after slicing, θ is the arc angle, R is the radius of the arc, $\bar{L}_f$ is the cord gage length measurement after slicing, f is the *sagitta* of the arc, $\bar{L}_{dev}$ is the length of the *sagitta* measuring device, and α is the coefficient of linear expansion, which is assumed to be $10e^{-6}$ for steel.

4.4. Residual stress measurement results and discussion

Fig. 7 depicts the residual stress measurement results for all cross sections sorted with ascending order of height (see Table 2). The residual stress predictions by Young [11] and ECCS [4] are also superimposed in the same figure for comparison purposes. It is observed that both top and bottom flange measurements provide fairly similar results for all cross sections. This is justifiable, given that the measurements were conducted in non-straightened members, where symmetry in the flange residual stresses is expected.

The results highlight that the assumption of parabolic residual stress distributions in hot-rolled wide flange sections is reasonable. Regardless of the geometry of the cross section, the web is mostly in compression, contrary to the model proposed by Galambos and Ketter [7]. Moreover, the results suggest that, qualitatively, cross sections with higher cross-sectional area, A, develop increased residual stresses in the flanges. This is consistent with observations by Spoorenberg [30]. The effect of the cross-sectional area on the residual stresses in the web appears to be less significant. In this case, residual stresses tend to increase with increased h/b_f. Referring to Figs. 7a and 7b, the ECCS [4] and the Young [11] models provide unrealistic results for light-weight cross sections, because they only rely on h/b_f and A_w/A_f, respectively. Moreover, according to the same figures, the Young model [11] is more accurate on deep cross sections with $(b_f t_w)/(d_w t_f) < 0.5$.

Fig. 8 shows comparisons of residual stress measurements on sections with nominally identical geometry but variable material yield strength (see Fig. 8a), manufacturing date and company (see Fig. 8b). For the former comparison, results of the present study (i.e., $f_{y,n}$ = 355 MPa) and Daddi and Mazzolani [32] (i.e., $f_{y,n}$ = 235 MPa) are shown in Fig. 8a for an IPE 200. Referring to Fig. 8a, decreased residual stresses are highlighted for the material with higher yield strength, contrary to available residual stress model assumptions (e.g., ECCS [4]). Comparisons of the IPE 360 section of the present study and the one by Spoorenberg [30], suggest the opposite. These results demonstrate that the material yield strength may not necessarily affect residual stresses [30].

Referring to Fig. 8b, the HEA 160 measurements of the present study are compared with those of the equivalent W6 × 20 US section from Dibley [22]. Although residual stresses in the flange do not substantially vary, this does not hold true for the web. This may be attributable to the manufacturing process of different manufacturers or the different quality control of steel production in the 1970s and the 2020s. The findings of Fig. 8 suggest that a new residual stress model is imperative.

5. Proposed residual stress model for hot-rolled wide flange steel members

5.1. Methodology

The residual stress model development is based on a constrained least square method that is applied to the collected residual stress data. The residual stress observation least squares are minimized to a model that is assumed to follow a parabolic curve [11,12]. The problem can be formulated as a quadratic program [58], according to Eq. (5). Referring to Eq. (5a), vector $\mathbf{x}$ comprises the optimization variables that minimize the objective function that is defined by matrix $\mathbf{P}$ and vector $\mathbf{q}$. A set of inequality and equality constraints need to be respected, as per Eq. (5b).

$$\text{minimize} \quad \frac{1}{2}\mathbf{x}^{\mathrm{T}}\mathbf{P}\mathbf{x} + \mathbf{q}^{\mathrm{T}}\mathbf{x} \tag{5a}$$

$$\text{subjected to} \quad \mathbf{G}\mathbf{x} \leq \mathbf{h} \text{ and } \mathbf{A}\mathbf{x} = \mathbf{b} \tag{5b}$$

The residual stress model of the flange and the web are described in Eqs. (6a) and (6b), respectively (see Fig. 1 for the coordinate system). Coefficients a and c introduced in Eq. (6) describe the residual stresses in the flange and web centers, respectively. Due to symmetry in the cross section, both flanges are assumed to develop the same residual stresses, given in Eq. (6a).

$$\sigma_{0,f}(x) = a + b(x - b_f/2)^2 \tag{6a}$$

$$\sigma_{0,w}(y) = c + d(y - h/2)^2 \tag{6b}$$

The sum of squares of the difference between the flange residual stress observations and the model of Eq. (6a) is given in Eq. (7a). This equation is rewritten as shown in Eq. (7b). By expanding the quadratic form of Eq. (7b), the final form for the residual stresses in the flanges is given in Eq. (7c). This form conforms with the quadratic program formulation, introduced in Eq. (5a). Following the same methodology, the formulation of the web residual stresses can be derived by accounting for the parabolic distribution of Eq. (6b). It should be noted that in cases where measured residual stresses are reported for both section flanges, the sum of least squares of the quadratic program of Eq. (7) considers both flanges:

$$\frac{1}{2}\sum_{i=1}^{n}[\sigma_{0,f}(x_i) - \sigma_{0,f}^{meas}(x_i)]^2 = \frac{1}{2}\sum_{i=1}^{n}[a + b(x_i - b_f/2)^2 - \sigma_{0,f}^{meas}(x_i)]^2 \tag{7a}$$

$$\frac{1}{2}\|\mathbf{Q}_{\mathrm{ab}}\mathbf{x}_{\mathrm{ab}} - \boldsymbol{\sigma}_{\mathrm{ab}}\|_2^2, \text{ where: } \mathbf{Q}_{\mathrm{ab}} = \begin{Bmatrix} 1 & (x_1 - b_f/2)^2 \\ 1 & (x_2 - b_f/2)^2 \\ \vdots & \vdots \\ 1 & (x_n - b_f/2)^2 \end{Bmatrix}, \mathbf{x}_{\mathrm{ab}} = \begin{Bmatrix} a \\ b \end{Bmatrix}, \text{ and } \boldsymbol{\sigma}_{\mathrm{ab}} = \begin{Bmatrix} \sigma_{0,f}^{meas}(x_1) \\ \sigma_{0,f}^{meas}(x_2) \\ \vdots \\ \sigma_{0,f}^{meas}(x_n) \end{Bmatrix} \tag{7b}$$

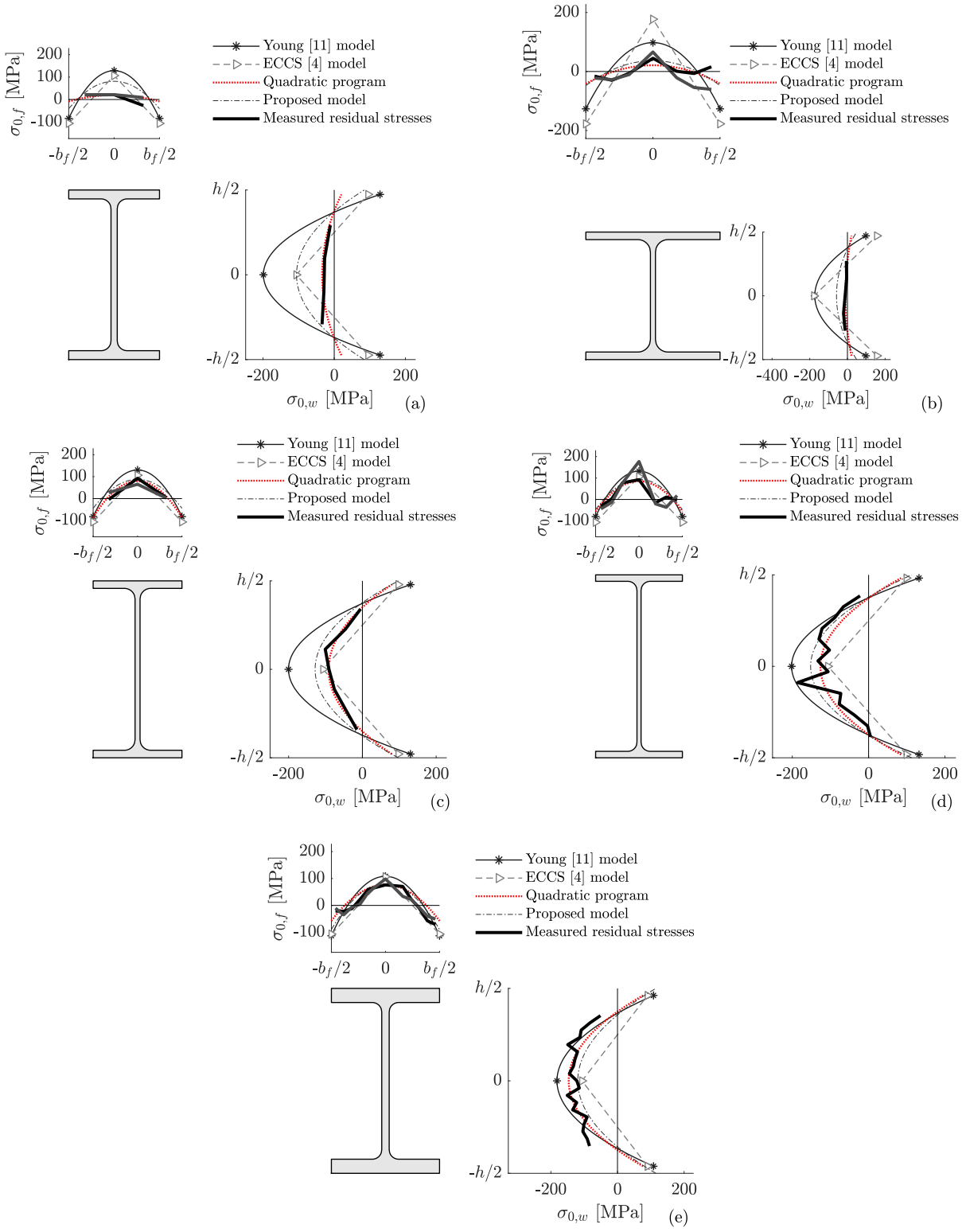

Fig. 7. Residual stress measurements: (a) IPE 120; (b) HEA 160; (c) IPE 200; (d) IPE 360; and (e) HEM 500.

$$\frac{1}{2}\mathbf{x}_{ab}^{T}\mathbf{P}_{ab}\mathbf{x}_{ab}+\mathbf{q}_{ab}^{T}\mathbf{x}_{ab},\ \text{where: } \mathbf{P}_{ab}=\mathbf{Q}_{ab}^{T}\mathbf{Q}_{ab},\ \text{and } \mathbf{q}_{ab}=-\mathbf{Q}_{ab}^{T}\boldsymbol{\sigma}_{ab}, \tag{7c}$$

where $\sigma_{0,f}^{meas}(x_i)$ is the flange residual stress measurement at location x_i, and n is the number of residual stress measurement points in the flange.

The constrained least square problem is subjected to force equilibrium and continuity constraints within the cross section. The force equilibrium is satisfied by constraining the sum of forces in the flanges and the web to equal zero, as shown in Eq. (8). It should be noted that the fillet radii is disregarded from the equilibrium and, therefore, from the formulation of the residual stress model. With regards to the continuity, it is imposed that residual stresses in the web-to-flange joint are continuous. This constraint considers the centerlines of the web and flange plates, as described in Eq. (9). Given the four coefficients of the residual stress model (see Eq. (6)) and the two equations that relate those (see Eqs. (8) and (9)), the development of the residual stress

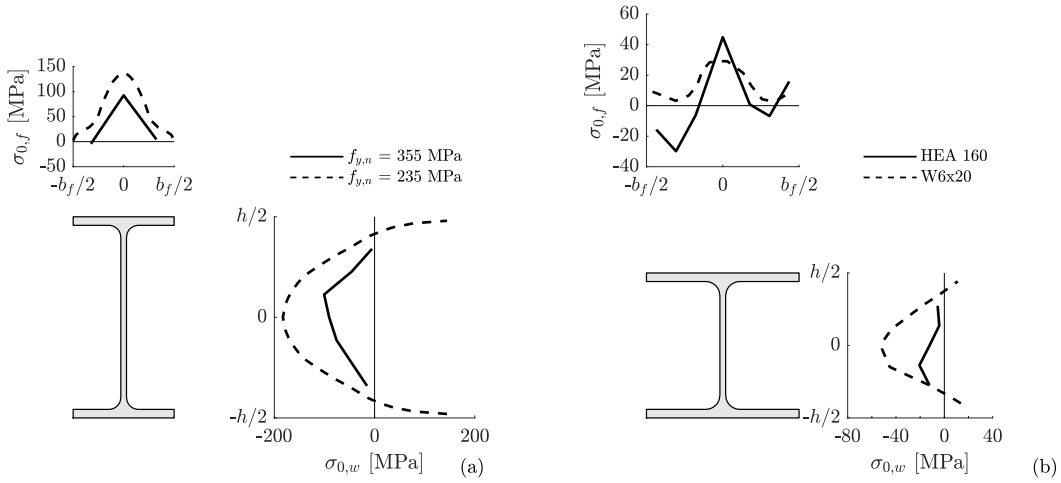

Fig. 8. Comparisons of residual stresses in cross sections with variable: (a) material yield strength; and (b) manufacturing practices.

model relies on coefficients a and c of Eq. (6).

$$F_f + F_w = 2t_f \int_0^{b_f} \sigma_{0,f}(x)\,dx + t_w \int_{t_f}^{h-t_f} \sigma_{0,w}(y)\,dy = 0 \rightarrow$$
$$2t_f b_f a + 2t_f \frac{b_f^3}{12} b + t_w(h-2t_f)c + t_w \frac{(h-2t_f)^3}{12} d = 0 \quad (8)$$

$$\sigma_{0,f}(b_f/2) = \sigma_{0,w}(h-t_f/2) \rightarrow$$
$$a = c + d(h-t_f)^2/4 \quad (9)$$

The results of the quadratic program are superimposed in the residual stress measurements of the present study in Fig. 7. It is observed that the proposed methodology provides an accurate representation of the residual stresses in the web and the flanges, regardless of the cross-sectional geometry. Therefore, the development of the residual stress model is based on the optimization results of the quadratic program.

5.2. Observed trends of the residual stress model parameters

Previous work has shown the influence of cross-sectional geometric parameters on residual stresses of hot-rolled wide flange sections. Among the influential parameters, the following prevail [4,7,11,12,36] : A_f, A_w, h, t_f, b_f, h/b_f, A, A_w/A_f, $(b_f/t_f)/(d_w/t_w)$. Statistical analysis on these geometric parameters highlighted that the most influential parameters on coefficients a and c of the quadratic program described in Eq. (6) are h, A and h/b_f for the flange and h/b_f for the web. These observations are in line with the discussion of Section 4.4.

Fig. 9 depicts the influence of these geometric parameters on the quadratic program coefficients a and c (see Figs. 9a-c and 9d, respectively). The dashed straight lines superimposed in these figures indicate the statistical trends within the range of applicability of the proposed model. These figures distinguish between data measurements on cross sections fabricated with both older and more recent manufacturing processes to acknowledge the potential improvement of quality control over time. Since there is lack of measurements between 1992 and 2010 (see Table 1), the data are distinguished in groups of *before 1992* and *after 2010*. Moreover, an additional dataset of all assembled data of Table 1 is examined. With regards to the quadratic program coefficient a, which describes the residual stresses at the flange center, it is qualitatively observed that for increased cross-sectional area, A, and height, h, residual stresses increase. This is in line with past observations [30] and may be attributed to the higher rate of cross-sectional differential cooling once the area of the cross section increases. Moreover, for increased h/b_f values, residual stresses in the flanges and the web increase (see Figs. 9b). Since h/b_f is almost perfectly collinear with A_w/A_f, this observation is in line with Young [11], while it opposes to the residual stress model of ECCS [4].

To give a quantitative sense on the highlighted statistical trends, the coefficient of determination, R^2, is calculated for the above independent (i.e., predictor) and dependent (i.e., response) variables. With regards to the h/b_f parameter, R^2 ranges between 0.3 and 0.4 for the response variable coefficients a and c of the quadratic program, respectively. R^2 increases by up to 10% in the *after 2010* subset compared to the full dataset. Referring to the predictor variables A and h, the coefficient of determination equals 0.5 and 0.7, respectively, for the *after 2010* subset for predicting the response variable coefficient a. The R^2 values decrease by nearly half in this case when the full dataset is considered. Due to lack of scientific evidence to support utilization of the *after 2010* dataset, the proposed residual stress model relies on all the collected data of Table 1.

5.3. Statistical analysis

The statistical trends discussed in Section 5.2 highlight that multiple linear regression analysis is suitable for the residual stress model development. Stepwise regression analysis is performed for this purpose [59], which is based on a combination of forward selection and backward elimination (i.e., bidirectional elimination). The regression analysis model is based on the most influential geometric characteristics of a cross section. Other than the significant predictor variables h, A and h/b_f, the model also includes the variables A_w/A, d_w/t_w, and t_f, as shown in Eq. (10). The predictor variables, $X = [h,\ A,\ h/b_f,\ A_w/A,\ d_w/t_w,\ t_f]$, are normalized (referred to as $\overline{X}$) as shown in Eq. (11). This normalization is applied so as the predictor variables are bounded within [-1 1]. In that way, the regression coefficients, β_i, indicate the significance of the predictor variable, X_i, they correspond to. The statistical significance of the regression model is not affected by this normalization, since the predictor variables are linearly modified.

$$y = \beta_0 + \beta_1 \cdot \overline{h} + \beta_2 \cdot \overline{A} + \beta_3 \cdot \overline{h/b_f} + \beta_4 \cdot \overline{A_w/A} + \beta_5 \cdot \overline{d_w/t_w} + \beta_6 \cdot \overline{t_f} + \epsilon \quad (10)$$

$$\overline{X_i} = 2 \cdot \frac{X_i - \min(X_i)}{\max(X_i) - \min(X_i)} - 1 \quad (11)$$

Where y is the response variable of interest (i.e., coefficients a and c), β_i are the regression coefficients, ϵ is the difference of the measured and the predicted response (i.e., regression model residual), and $\min(X_i)$ and $\max(X_i)$ are the minimum and maximum values of the predictor variable, X_i over the full dataset of Table 1, respectively.

The correlation matrix is constructed for the predictor variables of Eq. (10), so as variables with collinearity are not considered in the regression model. This matrix is not shown due to brevity. The

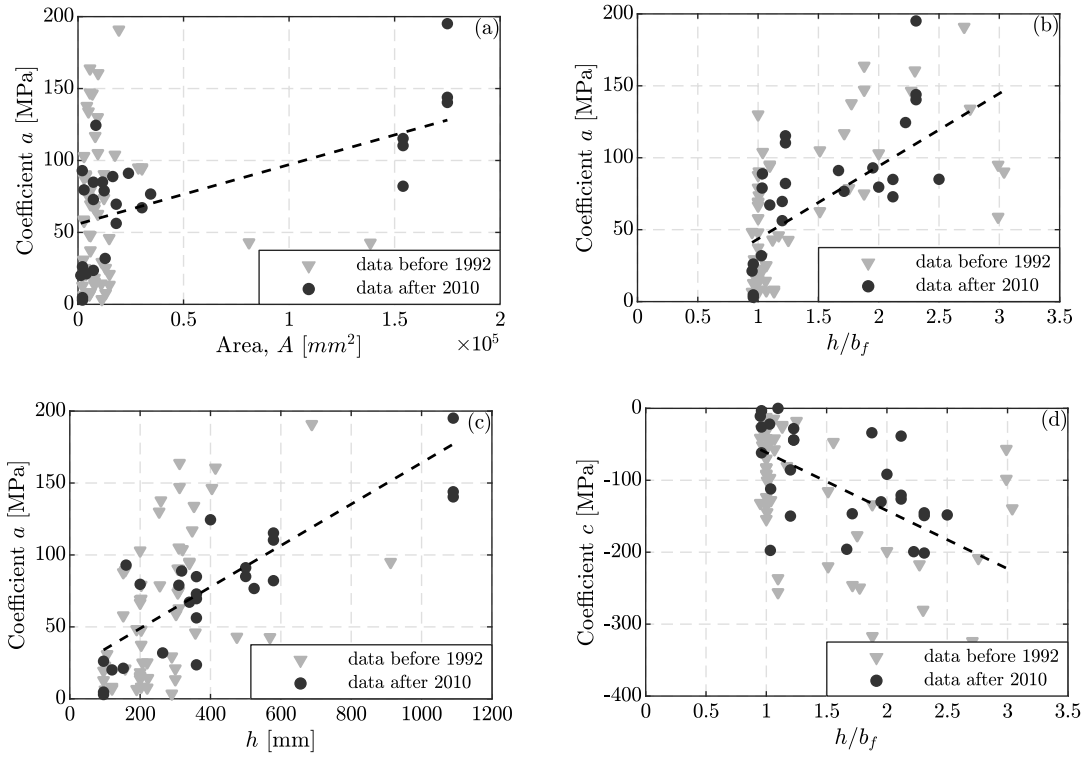

Fig. 9. Quadratic program coefficient trends over characteristic cross-sectional geometric properties: (a) Coefficient a versus A; (b) Coefficient a versus h/b_f; (c) Coefficient a versus h; and (d) Coefficient c versus h/b_f.

Pearson's linear correlation coefficients are calculated for this purpose. Among the significant predictor variables h, A and h/b_f, variable h is correlated with both A and h/b_f. Therefore, regardless of the significance of h, this variable is eliminated, since the model comprising both A and h/b_f is more significant, based on standard F-tests with a 95% confidence level.

Apart from the correlation coefficient checks, the quality of the multiple linear regression analysis is assessed based on the Gauss–Markov theory [59]. The discussion herein is based on the response variable coefficient a. Similar findings hold true for coefficient c but are not presented due to brevity.

Firstly, normality of the residuals should be respected in the regression analysis. This hypothesis is checked according to the Shapiro and Wilk test [60]. The p-value of 0.4 of the normality test confirms the assumption of the null hypothesis of the residual normality, based on a 5% significance level. This is visually supported by the quantile–quantile plot (i.e., QQ plot) illustrated in Fig. 10a. The data follow the theoretical dashed red straight line of linearity, while skewness in the data is not present. From the same figure, no data exceed the 95% confidence levels. Therefore, outliers are not part of the dataset utilized for the regression analysis.

Secondly, the assumption of homogeneity of variances should be verified. Fig. 10b depicts the raw residuals versus the fitted values. No evident relation is observed between the residuals and the fitted values. The constant variance with respect to the fitted values entails homogeneity of variances. From the same figure, the mean of residuals is practically zero, as also confirmed by a statistical t-test with a 95% confidence level.

Thirdly, no correlation was observed between the residuals and the predictor variables. A characteristic example is illustrated in Fig. 10c for the predictor variable h/b_f. The constant variance between the residuals and the predictor variable implies no correlation among the residuals.

5.4. Proposed residual stress model coefficients

The coefficients a and c of the proposed residual stress model are given in Eqs. (12) and (13), respectively. These coefficients in combination with the constraints imposed in Eqs. (8) and (9) define the coefficients of the proposed residual stress model (see Eq. (6)). The statistical analysis in combination with the exclusion of variables with increased collinearity highlighted that coefficient a of the residual stress model is described by h/b_f and A, while coefficient c by h/b_f. The standard deviations of the proposed residual stress model coefficients are also given in Eqs. (12) and (13). The calculated R^2 are 0.4 and 0.3 for coefficient a and c, respectively. The relatively low R^2 values are attributed to the significant variability in the way residual stresses form in hot-rolled wide flange sections, as elaborated previously. The F-test of the significance of the proposed equations leads to p-values of $2e^{-9}$ and $1e^{-6}$, respectively. Therefore, the proposed regression model is robust. It should be noted that by utilizing residual stress data measurements conducted after 2010, the above p-values decrease considerably. Even if there is an indication that the difference in quality control and fabrication practices matters in how residual stress form, the collected data are not adequate to justify this. Therefore, the full dataset is employed for the model development. The experimental data utilized for the derivation of Eqs. (12) and (13) are characterized by 1320 mm^2 $\leq A \leq$ 175 000 mm^2 and $0.95 \leq h/b_f \leq 3.0$. The bounds of these variables serve for denormalizing the predictor variables of Eqs. (12) and (13), according to Eq. (11).

$$a = 107 + 51 \cdot \overline{h/b_f} + 20 \cdot \overline{A},\ \sigma_a = 37 \text{ MPa} \tag{12}$$

$$c = -(142 + 84 \cdot \overline{h/b_f}),\ \sigma_c = 81 \text{ MPa} \tag{13}$$

To explore the potential influence of f_y on the residual stresses, the statistical analyses described herein were repeated for the residual stress data of Table 1. For this purpose, the measured residual stress data were normalized with respect to f_y, similarly to the ECCS model [4]. The results showed that the statistical significance of this

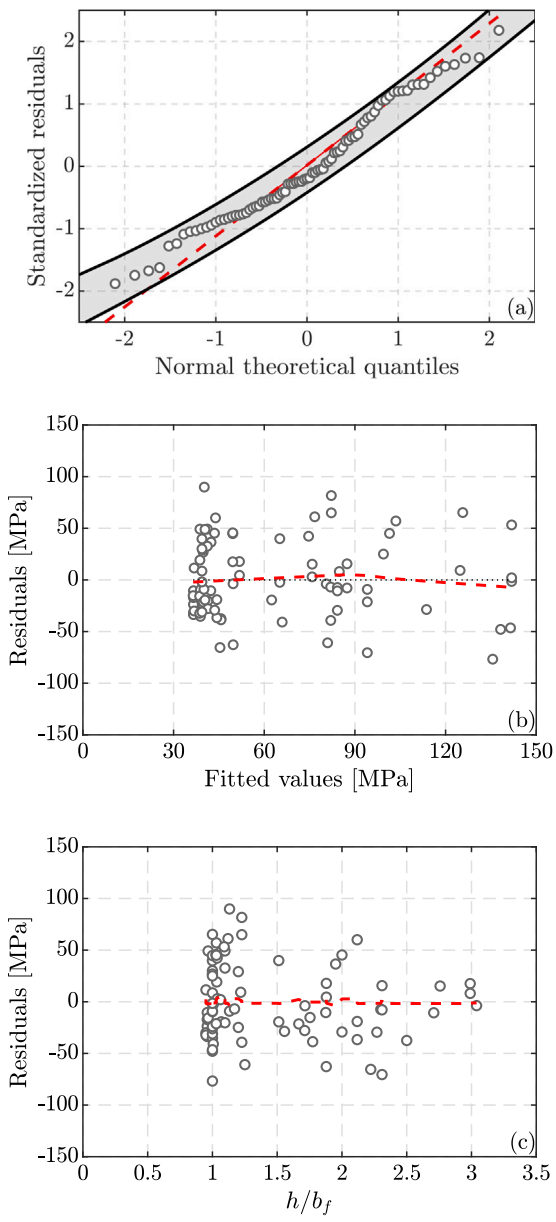

Fig. 10. Regression analysis residuals of coefficient a of the residual stress model: (a) regression analysis quantile–quantile plot; (b) regression analysis residuals versus fitted values; and (c) regression analysis residuals versus h/b_f.

residual stress model is significantly lower compared to the proposed one that disregards f_y, similarly to Young [11]. This confirms that there is no pertinent evidence that f_y influences the built-in residual stresses in hot-rolled wide flange cross sections.

5.5. Evaluation of the proposed residual stress model

The proposed residual stress model is evaluated based on the k-fold cross-validation method [61]. Given the limited number of collected residual stress data, this method is valuable since the full dataset is utilized as training and test dataset. The dataset is divided into k folds of approximately equal size. All possible combinations of $k-1$ folds are used as training subsets and the remaining fold per combination is used as test subset. A typical value for this method is $k = 10$, leading to a training-to-test subset ratio of 90/10 [61]. Based on this method, the collected residual stress dataset is divided randomly into 10 subsets. This leads to 10 different residual stress models that are based on the stepwise regression method applied in the training subsets. Therefore, the model is trained based on 77 data and evaluated based on the remaining 8 data for each of the 10 combinations of subsets.

The regression model coefficients for all k-fold models are given in Fig. 11. Interestingly, the coefficients are insensitive to the k-fold models and they match those of the full-dataset model. Similar findings hold true for the standard deviations, R^2 and the p-values of the proposed full-dataset and all k-fold models.

Fig. 12 shows the L1-norms for the difference between the measured residual stresses and characteristic residual stress models (see Eq. (1)) for the test subset of a randomly selected k-fold model (i.e., k-fold model 9). The L1-norms are normalized to the maximum L1-norm value of available residual stress models (i.e., [4,7,11,12,36]). It is observed that the k-fold model provides practically the same accuracy with the proposed model, both for the flange and the web residual stresses (see Fig. 12a and Fig. 12b, respectively). This suggests that the proposed residual stress model is not biased towards the selected dataset. With regards to the flange residual stresses, the Young [11] and the ECCS [4] models provide similar accuracy. For nearly all test subset data of the 9th k-fold model, the proposed residual stress model reduces the error in the flanges by a factor of at least two, compared to available models in literature. This is particularly important, because the buckling resistance of a steel member is mainly provided by the flanges of its cross section [38]. Regarding the web residual stresses, the ECCS model [4] provides similar accuracy with the proposed model for the selected test subset. The accuracy of the proposed model in predicting residual stresses in hot-rolled wide flange sections is, characteristically, illustrated in Fig. 7.

Fig. 13 shows the normalized L1-norms for the difference between the measured and characteristic residual stress models for the full dataset. The test data are sorted with ascending order of cross-sectional aspect ratio, h/b_f. The quadratic program normalized L1-norms are also superimposed in the same figure for reference. It is observed that the normalized L1-norms for the difference between the measured residual stresses and the quadratic program optimized distributions is not infinitesimal. This is attributed to the fact that residual stresses may not always follow a parabolic distribution, either because of the measuring accuracy or because of the nature of their formation (e.g., see Fig. 7c). To give a quantitative sense in that error, the mean of the calculated L1-norms over the full database equals 0.1 and 0.05 for the flange and the web, respectively. Therefore, a source of error attributable to this aspect is expected in the proposed residual stress model that is based on the quadratic program.

Referring to Fig. 13, the proposed model for the flanges and the web leads to similar accuracy with the quadratic program for most of the experimental data, regardless of h/b_f. The Young model [11] error reduces with increasing h/b_f, while the ECCS model [4] is not accurate for h/b_f values that are close to the database bounds. To quantify the residual stress model errors, Fig. 14 shows the histogram of the calculated L1-norms for the proposed and the ECCS [4] residual stress models. Superimposed are the probability density functions of log-normal distributions that are fitted to the histogram. With regards to the residual stress distributions in the flange (see Fig. 14a), the mean of the log-normal distribution of the proposed model equals 0.14 and the one of the ECCS model [4] equals 0.23. Similar observations hold true for the web (see Fig. 14b). Therefore, the proposed model reduces by nearly 60% the error in predicting residual stresses in the flange and the web compared to the widely used ECCS [4] model. Moreover, the proposed model reduces by two times the variance of the error for the web and four times for the flanges.

6. Summary and conclusions

This paper proposes a new residual stress model for wide flange hot-rolled steel cross sections. To achieve this, a residual stress measurement dataset is first collected and supplemented by additional

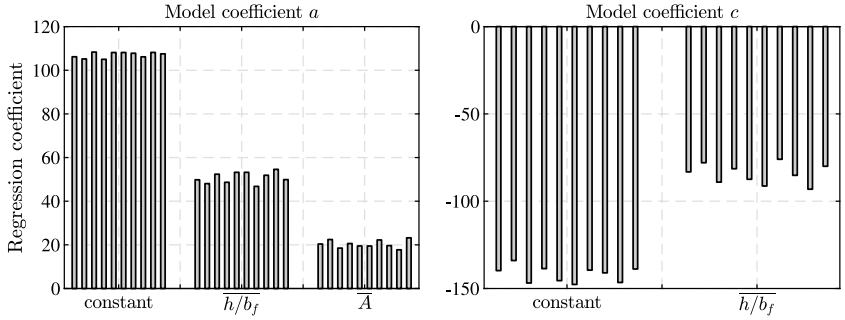

Fig. 11. Regression analysis coefficients for the predictor variables of the residual stress model coefficients a and c for all regression models of the k-fold method.

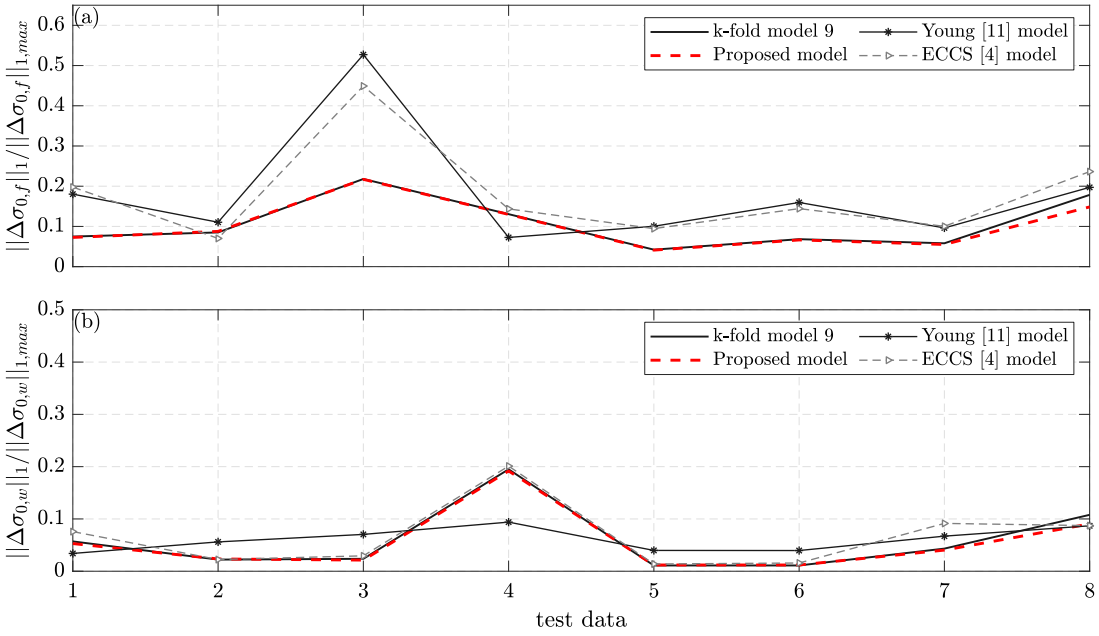

Fig. 12. Normalized L1-norms for the proposed, the 9th k-fold, the Young [11] and the ECCS [4] residual stress models for the test data of the 9th k-fold model: (a) flange; and (b) web distribution.

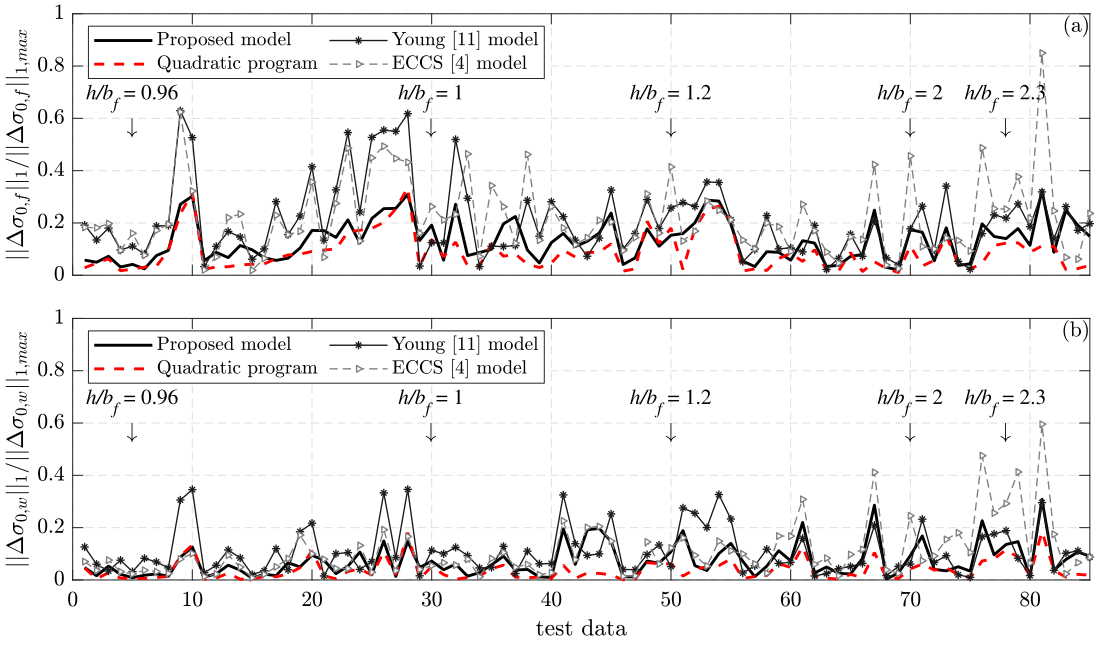

Fig. 13. Normalized L1-norms for the proposed, the quadratic program, the Young [11] and the ECCS [4] residual stress models for the full dataset: (a) flange; and (b) web distribution.

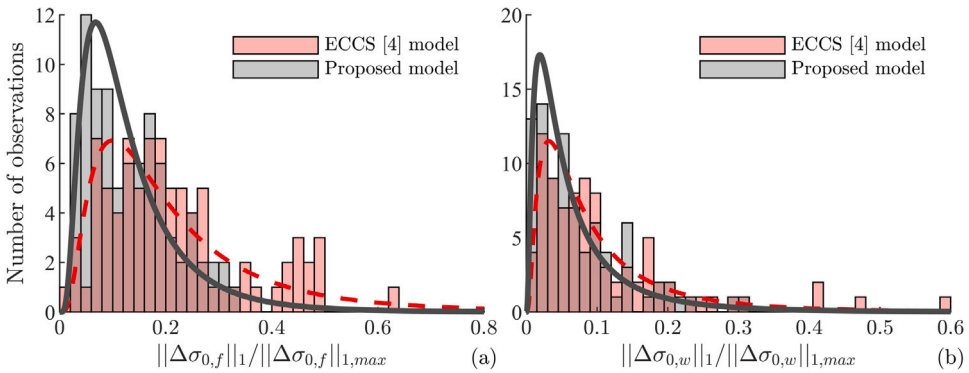

Fig. 14. Distribution of the normalized L1-norms for the proposed and the ECCS [4] residual stress models for the full dataset: (a) flange; and (b) web distribution.

measurements for geometries where data are lacking in. The assembled dataset, which is made publicly available (https://resslab-hub.epfl.ch/) includes 85 data on members fabricated between 1950 and 2021 and comprises variable cross-sectional geometries and material properties. A constrained optimization problem is formulated to best describe the residual stress measurements for the flanges and the web. The optimization problem is based on minimizing the least squares of differences between the assumed parabolic distributions and the measurements. Constraints for force equilibrium and continuity in the residual stresses of the web and the flanges are applied to the optimization problem. A residual stress model is then developed based on the assembled data and statistical analyses on the residual stress distributions developed by the optimization method. The proposed model is evaluated based on the collected dataset and is compared with available models in the literature. The primary findings of the present study are summarized as follows:

- Statistical analyses on the collected data revealed that there is no pertinent evidence that the material yield strength, f_y, affects the residual stresses in hot-rolled wide flange steel cross sections conditioned that the residual stresses do not exceed f_y.
- The residual stress model by Galambos and Ketter [7], is not valid for stocky sections where the web is primarily in compression and residual stresses follow a parabolic distribution. On the other hand, the Young model [11] provides reasonable predictions for sections with $(b_f t_w)/(d_w t_f) < 0.5$ that are usually utilized for steel beams in building applications. The models by Bradford and Trahair [36] and ECCS [4], are not generally representative of residual stresses in steel cross sections, since they rely on f_y and not on geometric features of the cross section. The Szalai and Papp model [12] leads to erroneous residual stress distributions in the web for stocky sections, because it assumes that the Wagner coefficient is equal to zero.
- Among the available residual stress models in the literature, the residual stress model by Young [11] describes best the residual stresses in hot-rolled wide flange cross sections with $h/b_f > 1.5$. For cross sections with $h/b_f \leq 1.5$, there is no consensus in which model is more representative.
- The peak tensile residual stress in the cross-sectional flanges is justified with high statistical significance by the cross-sectional area, A, and height-to-width ratio, h/b_f. The peak compressive residual stress in the cross-sectional web is best described by h/b_f. The associated coefficients of determination of the developed multiple linear regression models are 0.4 and 0.3, respectively. Although these statistical parameters are almost double when the developed residual stress model considers data of members fabricated with modern fabrication techniques and quality control, there is not scientific basis to justify a model that considers only this subset.
- The proposed residual stress model for hot-rolled wide flange steel members leads to similar accuracy with optimally fitted parabolic distributions to residual stress measurements from the flanges and the web of hot-rolled cross sections. Compared to the ECCS model, the proposed residual stress model reduces the error in predicting residual stresses in the flanges and the web by nearly 70%. Other than the mean of error, the variance of error is also decreased by a factor of four and two for the flanges and the web, respectively.

CRediT authorship contribution statement

Andronikos Skiadopoulos: Conceptualization, Investigation, Methodology, Visualization, Writing – original draft, Writing – review & editing. **Albano de Castro e Sousa:** Conceptualization, Investigation, Methodology, Visualization, Writing – original draft, Writing – review & editing. **Dimitrios G. Lignos:** Methodology, Conceptualization, Funding acquisition, Project administration, Supervision, Validation, Writing – original draft, Writing – review & editing.

Declaration of competing interest

The authors declare that they have no known competing financial interests or personal relationships that could have appeared to influence the work reported in this paper.

Data availability

We have provided a link to a public repository where all data will be made publicly available once the manuscript is accepted for publication.

Acknowledgments

The present study is based on work supported by an EPFL, Switzerland internal grant. The financial support is gratefully acknowledged. The authors would like to sincerely thank Professors Raffaele Landolfo and Mario D'Aniello from University of Naples Federico II for retrieving priceless textbooks with available residual stress measurements, Mr. Gabriele Falconi (former Master's student of EPFL), for his invaluable contribution in residual stress measurements at EPFL, and Dr. Nenad Bijelić for providing extensive feedback on the final version of the manuscript. Any opinions, findings, and conclusions or recommendations expressed in this paper are those of the authors and do not necessarily reflect the views of sponsors.

References

[1] L.S. Beedle, L. Tall, Basic column strength, J. Struct. Div. 86 (7) (1960) 139–173, Publisher: American Society of Civil Engineers.

[2] C.C. Weng, T. Pekoz, Residual stresses in cold-formed steel members, J. Struct. Eng. 116 (6) (1990) 1611–1625, http://dx.doi.org/10.1061/(ASCE)0733-9445(1990)116:6(1611), Publisher: American Society of Civil Engineers.

[3] E. Mas, C.E. Massonnet, Part prise par la belgique dans les recherches experimentales de la convention europeenne des associations de la construction metallique sur le flambement centriques des barres en acier doux, Acier-Stahl-Steel 9 (1966) 393–400, Publisher: Centre belgo-luxembourgeois d'information de l'acier.

[4] ECCS, Manual on Stability of Steel Structures. Part 2.2 Mechanical Properties and Residual Stresses, European Convention for Constructional Steelwork (ECCS), Bruxelles, 1976.

[5] L.S. Beedle, A.W. Huber, Residual Stress and the Compressive Properties of Steel - a Summary Report, Tech. Rep. 220A.27, Fritz Laboratory, Lehigh University, Bethlehem, PA, USA, 1957.

[6] D. Feder, G.C. Lee, Residual Stress and the Strength of Members of High Strength Steel, Tech. Rep. 269.2, Fritz Laboratory, Lehigh University, Bethlehem, PA, USA, 1959.

[7] T.V. Galambos, R.L. Ketter, Columns under combined bending and thrust, J. Eng. Mech. Div. 85 (2) (1959) 1–30, http://dx.doi.org/10.1061/JMCEA3.0000084, Publisher: American Society of Civil Engineers.

[8] A.W. Huber, Residual Stresses in Wide-Flange Beams and Columns, Tech. Rep. 220A.25, Fritz Laboratory, Lehigh University, Bethlehem, PA, USA, 1956.

[9] A.W. Huber, L.S. Beedle, Residual Stress and the Compressive Strength of Steel, Tech. Rep. 220A.9, Fritz Laboratory, Lehigh University, Bethlehem, PA, USA, 1953.

[10] R.L. Ketter, The influence of residual stress on the strength of structural members, Weld. Res. Counc. Bull. Ser. 44 (1) (1958) 1–11, Publisher: Welding Research Council (US).

[11] B. Young, Residual stresses in hot rolled members, IABSE Rep. Work. Commiss. 23 (1) (1975) 25–38, http://dx.doi.org/10.5169/SEALS-19798, Publisher: International Association for Bridge and Structural Engineering (IABSE).

[12] J. Szalai, F. Papp, A new residual stress distribution for hot-rolled I-shaped sections, J. Construct. Steel Res. 61 (6) (2005) 845–861, http://dx.doi.org/10.1016/j.jcsr.2004.12.004, Publisher: Elsevier.

[13] G.A. Alpsten, Thermal Residual Stresses in Hot-Rolled Steel Members, Tech. Rep. 337.3, Fritz Laboratory, Lehigh University, Bethlehem, PA, USA, 1968.

[14] M. Abambres, W.-M. Quach, Residual stresses in steel members: a review of available analytical expressions, Int. J. Struct. Integr. 7 (1) (2016) 70–94, http://dx.doi.org/10.1108/IJSI-12-2014-0070, Publisher: Emerald Publishing.

[15] L.S. Beedle, The Influence of Residual Stress on Column Strength - a Proposed Pilot Investigation, Fritz Laboratory, Lehigh University, Bethlehem, PA, USA, 1951.

[16] J. Strating, H. Vos, Computer simulation of the e.c.c.s. buckling curve using a monte-carlo method, Heron 19 (2) (1973) 1–38, Publisher: Delft University of Technology.

[17] M.G. Lay, R. Ward, Residual stresses in steel sections, J. Austr. Inst. Steel Constr. 3 (3) (1969) 2–21, Publisher: Australian Institute of Steel Construction.

[18] S. Shayan, K.J.R. Rasmussen, H. Zhang, Probabilistic modelling of residual stress in advanced analysis of steel structures, J. Construct. Steel Res. 101 (2014) 407–414, http://dx.doi.org/10.1016/j.jcsr.2014.05.028, Publisher: Elsevier.

[19] C.-P. Lamarche, R. Tremblay, Seismically induced cyclic buckling of steel columns including residual-stress and strain-rate effects, J. Construct. Steel Res. 67 (9) (2011) 1401–1410, http://dx.doi.org/10.1016/j.jcsr.2010.10.008, Publisher: Elsevier.

[20] P.M.M. Vila Real, R. Cazeli, L. Simões da Silva, A. Santiago, P. Piloto, The effect of residual stresses in the lateral-torsional buckling of steel I-beams at elevated temperature, J. Construct. Steel Res. 60 (3) (2004) 783–793, http://dx.doi.org/10.1016/S0143-974X(03)00143-3, Publisher: Elsevier.

[21] S. Quayyum, T. Hassan, Initial residual stresses in hot-rolled wide-flange shapes: A computational technique and influence on structural performances, J. Struct. Eng. 143 (5) (2017) 04017013, http://dx.doi.org/10.1061/(ASCE)ST.1943-541X.0001739, Publisher: American Society of Civil Engineers.

[22] J.E. Dibley, Lateral torsional buckling of I-sections in grade 55 steel, Proc. Inst. Civ. Eng. 43 (4) (1969) 599–627, http://dx.doi.org/10.1680/iicep.1969.7315, Publisher: Institution of Civil Engineers.

[23] K. Mathur, L.A. Fahnestock, T. Okazaki, M.J. Parkolap, Impact of residual stresses and initial imperfections on the seismic response of steel moment frames, J. Struct. Eng. 138 (7) (2012) 942–951, http://dx.doi.org/10.1061/(ASCE)ST.1943-541X.0000512, Publisher: American Society of Civil Engineers.

[24] A.Y.-C. Lu, G. MacRae, Residual stress effects on the seismic performance of low-rise steel frames, in: Proceedings of the Ninth Pacific Conference on Earthquake Engineering: Building an Earthquake-Resilient Society, New Zealand Society for Earthquake Engineering, Inc., Wellington, New Zealand, University of Auckland, Auckland, New Zealand, 2011, pp. 1–7.

[25] A.W. Huber, The Influence of Residual Stress on the Instability of Columns, Tech. Rep. 220A.22, Fritz Laboratory, Lehigh University, Bethlehem, PA, USA, 1956.

[26] AWS, Structural Welding Code—Steel, Tech. Rep.ANSI/AWS D1.1:2010, American Welding Society, Miami, FL, USA., 2010.

[27] AISC, Code of Standard Practice for Steel Buildings and Bridges, Tech. Rep. ANSI/AISC 303-05, American Institute of Steel Construction, Chicago, IL, USA, 2000.

[28] CEN, EN 1993-1-8: Eurocode 3: Design of Steel Structures – Part 1-8: Design of Joints, Tech. Rep., European Committee for Standardization, Brussels, Belgium, 2005.

[29] G.A. Alpsten, Residual stresses, yield stress, and column strength of hot-rolled and roller-straightened steel shapes, in: Proceedings IABSE Colloquium: on Column Strength, Paris, International Association for Bridge and Structural Engineering (IABSE), 1975, pp. 39–59, http://dx.doi.org/10.5169/SEALS-19799.

[30] R. Spoorenberg, H. Snijder, J. Hoenderkamp, Experimental investigation of residual stresses in roller bent wide flange steel sections, J. Construct. Steel Res. 66 (6) (2010) 737–747, http://dx.doi.org/10.1016/j.jcsr.2010.01.017, Publisher: Elsevier.

[31] R. Spoorenberg, H. Snijder, J. Hoenderkamp, Proposed residual stress model for roller bent steel wide flange sections, J. Construct. Steel Res. 67 (6) (2011) 992–1000, http://dx.doi.org/10.1016/j.jcsr.2011.01.009, Publisher: Elsevier.

[32] I. Daddi, F.M. Mazzolani, Determinazione sperimentale delle imperfezioni strutturali nei profilati di acciaio, Costr. Met. 5 (1971) 3–23.

[33] F. Mazzolani, Buckling curves of hot-rolled steel shapes with structural imperfections, IABSE Rep. Work. Commiss. 23 (1) (1975) 152–161, Publisher: International Association for Bridge and Structural Engineering (IABSE).

[34] Y. Fukumoto, Y. Itoh, M. Kubo, Strength variation of laterally unsupported beams, J. Struct. Div. 106 (1) (1980) 165–181, http://dx.doi.org/10.1061/JSDEAG.0005334, Publisher: American Society of Civil Engineers.

[35] Y. Fukumoto, Y. Itoh, Statistical study of experiments on welded beams, J. Struct. Div. 107 (1) (1981) 89–103, http://dx.doi.org/10.1061/JSDEAG.0005639, Publisher: American Society of Civil Engineers.

[36] M.A. Bradford, N.S. Trahair, Inelastic buckling of beam-columns with unequal end moments, J. Construct. Steel Res. 5 (3) (1985) 195–212, http://dx.doi.org/10.1016/0143-974X(85)90003-3, Publisher: Elsevier.

[37] R. Spoorenberg, H. Snijder, L.-G. Cajot, M. May, Experimental investigation on residual stresses in heavy wide flange QST steel sections, J. Construct. Steel Res. 89 (2013) 63–74, http://dx.doi.org/10.1016/j.jcsr.2013.06.009, Publisher: Elsevier.

[38] C. Jez-Gala, Residual stresses in rolled I-sections, Proc. Inst. Civ. Eng. 23 (3) (1962) 361–378, http://dx.doi.org/10.1680/iicep.1962.10874, Publisher: Institution of Civil Engineers.

[39] Y. Fujita, The Magnitude and Distribution of Residual Stress, Tech. Rep. 220A.20, Fritz Laboratory, Lehigh University, Bethlehem, PA, USA, 1955.

[40] L. Subramanian, D.W. White, Resolving the disconnects between lateral torsional buckling experimental tests, test simulations and design strength equations, J. Construct. Steel Res. 128 (2017) 321–334, http://dx.doi.org/10.1016/j.jcsr.2016.08.009, Publisher: Elsevier.

[41] C. Rebelo, N. Lopes, L. Simões da Silva, D. Nethercot, P.M.M. Vila Real, Statistical evaluation of the lateral–torsional buckling resistance of steel I-beams, part 1: variability of the eurocode 3 resistance model, J. Construct. Steel Res. 65 (4) (2009) 818–831, http://dx.doi.org/10.1016/j.jcsr.2008.07.016, Publisher: Elsevier.

[42] AISC, Specification for Structural Steel Buildings, Tech. Rep. ANSI/AISC 360-16, American Institute of Steel Construction, Chicago, IL, USA, 2016.

[43] L. Schaper, T. Tankova, L. Simões da Silva, M. Knobloch, A novel residual stress model for welded I-sections, J. Construct. Steel Res. 188 (2022) 107017, http://dx.doi.org/10.1016/j.jcsr.2021.107017, Publisher: Elsevier.

[44] A. Skiadopoulos, A. de Castro e Sousa, D.G. Lignos, Database of Residual Stress Measurements on Hot-Rolled Wide Flange Steel Cross Sections, Zenodo, 2023, http://dx.doi.org/10.5281/zenodo.7677600.

[45] P.F. Adams, M.G. Lay, T.V. Galambos, EXperiments on High Strength Steel Members, Tech. Rep. 297.8, Fritz Laboratory, Lehigh University, Bethlehem, PA, USA, 1964.

[46] J. Brozzetti, G.A. Alpsten, L. Tall, Residual Stresses in a Heavy Rolled Shape 14WF730, Tech. Rep. 337.10, Fritz Laboratory, Lehigh University, Bethlehem, PA, USA, 1970.

[47] C. Albert, H.S. Essa, D.J.L. Kennedy, Distortional buckling of steel beams in cantilever-suspended span construction, Can. J. Civil Eng. 19 (5) (1992) 767–780, http://dx.doi.org/10.1139/l92-088, Publisher: Canadian Science Publishing.

[48] K. Auger, Conception Parasismique Des Contreventements Concentriques En Treillis À Segments Multiples Combinés Aux Poteaux Gravitaires (Ph.D. thesis), Département des génies Civil, Géologique et des Mines École Polytechnique de Montréal, 2017.

[49] A. de Castro e Sousa, D.G. Lignos, Residual Stress Measurements of European Hot-Rolled I-Shaped Steel Profiles, Tech. Rep. 231302, Ecole Polytechnique Federale de Lausanne, Lausanne, 2017.

[50] P.F. Dux, S. Kitipornchai, Inelastic beam buckling experiments, J. Construct. Steel Res. 3 (1) (1983) 3–9, http://dx.doi.org/10.1016/0143-974X(83)90011-1, Publisher: Elsevier.

[51] D. Sonck, R.V. Impe, G. University, Study of residual stresses in I-section members and cellular members, in: Proceedings of the Annual Stability Conference Structural Stability Research Council St. Louis, Missouri, Curran Associates, Inc., St. Louis, MO, USA, 2013, pp. 584–602.

[52] T. Tankova, F. Rodrigues, C. Leitão, C. Martins, L. Simões da Silva, Lateral-torsional buckling of high strength steel beams: Experimental resistance, Thin-Walled Struct. 164 (2021) 107913, http://dx.doi.org/10.1016/j.tws.2021.107913, Publisher: Elsevier.

[53] N. Tebedge, G. Alpsten, L. Tall, Residual-stress measurement by the sectioning method: A procedure for residual-stress measurements by the sectioning method is described. Two different hole-drilling methods were performed and the results are compared, Exp. Mech. 13 (2) (1973) 88–96, http://dx.doi.org/10.1007/BF02322389, Publisher: Springer.

[54] W.W. Luxion, B.G. Johnston, Plastic behavior of wide-flange beams, Weld. J. 27 (11) (1948) 538–554, Publisher: American Welding Society.

[55] N.S. Rossini, M. Dassisti, K.Y. Benyounis, A.G. Olabi, Methods of measuring residual stresses in components, Mater. Des. 35 (2012) 572–588, http://dx.doi.org/10.1016/j.matdes.2011.08.022, Publisher: Elsevier.

[56] F.A. Kandil, J.D. Lord, A.T. Fry, P.V. Grant, A Review of Residual Stress Measurement Methods – a Guide to Technique Selection, Tech. rep., National Physical Laboratory Materials Centre, Teddington, UK, 2001.

[57] R.D. Ziemian (Ed.), Guide to Stability Design Criteria for Metal Structures, 6th ed., John Wiley & Sons, Hoboken, N.J, 2010, OCLC.

[58] S. Boyd, L. Vandenberghe, Convex Optimization, Cambridge University Press, 2004.

[59] S. Chatterjee, A.S. Hadi, Regression Analysis By Example, Wiley, Hoboken, NJ, 2015.

[60] S.S. Shapiro, M.B. Wilk, An analysis of variance test for normality (complete samples), Biometrika 52 (3–4) (1965) 591–611, http://dx.doi.org/10.1093/biomet/52.3-4.591, Publisher: Oxford University Press.

[61] G. James, D. Witten, T. Hastie, R. Tibshirani, an introduction to statistical learning, Springer Texts in Statistics, vol. 103, Springer New York, New York, NY, USA, 2013, http://dx.doi.org/10.1007/978-1-4614-7138-7.